Alexandria Engineering Journal (2022) 61, 6129–6138

HOSTED BY

ELSEVIER

Alexandria University

Alexandria Engineering Journal

www.elsevier.com/locate/aej
www.sciencedirect.com

Overlooked pitfalls in CaO carbonation kinetics studies nearby equilibrium: Instrumental effects on calculated kinetic rate constants

Juan Arcenegui-Troya [a,1,*], Jonatan D. Durán-Martín [a,1], Antonio Perejón [a,b], José M. Valverde [c], Luis A. Pérez Maqueda [a,*], Pedro E. Sánchez Jiménez [a,b,*]

[a] *Instituto de Ciencia de Materiales de Sevilla, C.S.I.C.-Universidad de Sevilla, C. Américo Vespucio n°49, 41092 Sevilla, Spain*
[b] *Departamento de Química Inorgánica, Facultad de Química, Universidad de Sevilla, Sevilla, Spain*
[c] *Faculty of Physics, University of Seville, Avenida Reina Mercedes s/n, Sevilla, Spain*

Received 26 August 2021; revised 27 October 2021; accepted 17 November 2021
Available online 02 December 2021

KEYWORDS

Energy Storage;
Calcium-Looping;
Concentrated Solar Power;
CO_2 capture, Kinetics;
Calcium Oxide

Abstract Due to its technological applications, such as CO_2 capture, CaO carbonation kinetics has been extensively studied using a wide array of methods and experimental conditions. A complete understanding of carbonation kinetics is key to optimizing the operating conditions as well as to correctly design the carbonation reactor. However, there is yet no consensus on the reaction model and kinetic parameters that can best describe the CaO carbonation reaction. For instance, the value of the activation energy proposed in different works can vary up to 300%. In this work, we demonstrate that the strong influence of the thermodynamic equilibrium on CaO carbonation kinetics demands careful control of the experimental conditions to obtain meaningful kinetic parameters. Specifically, we explore the influence of three experimental parameters on carbonation kinetics: the gas flow rate, the CO_2 partial pressure and the time required to fill the reactor after a gas change. We demonstrate that disregarding these aspects may lead to bogus conclusions on reaction kinetics, which could partly explain the considerable discrepancies found in the literature. The conclusions of this work are not only applicable to the process and experimental setup studied here but also to any study that involves the use of gas flow to drive a reaction.

1. Introduction

The rising CO_2 emission levels are aggravating the effects of global warming [1]. The Calcium-Looping (CaL) process, based on the highly reversible carbonation of CaO, has been long advocated as a post-combustion CO_2 capture technology to reduce the CO_2 content in the flue gas emitted by fossil fuel

* Corresponding authors at: Instituto de Ciencia de Materiales de Sevilla, C.S.I.C.-Universidad de Sevilla, C. Américo Vespucio n°49, 41092 Sevilla, Spain (P.E. Sánchez Jiménez).
E-mail addresses: jjarcenegui@icmse.csic.es (J. Arcenegui-Troya), maqueda@cica.es (L.A. Pérez Maqueda), pedro.enrique@icmse.csic.es (P.E. Sánchez Jiménez).
[1] Juan. A-T and Jonatan D-M. contributed equally to this work.
Peer review under responsibility of Faculty of Engineering, Alexandria University.

https://doi.org/10.1016/j.aej.2021.11.043

plants or cement manufacture facilities [2,3]. The low cost and lack of toxicity of limestone constitute important advantages over other Carbon Capture and Sequestration technology (CCS) systems, such as solvent scrubbing, mineralization and solid low-temperature adsorbents [2,4]. Furthermore, the CaL process is currently being explored as a thermochemical energy storage technology to be integrated with Concentrating Solar Power (CSP) plants [5–7]. In the CSP-CaL scheme, solar radiation is used to drive the endothermic decomposition of $CaCO_3$ into CaO and the energy thus stored could be recovered afterwards through the reverse exothermic solid–gas reaction between CaO and CO_2 in a carbonator reactor [5,8].

A comprehensive understanding of carbonation and calcination kinetics is crucial to optimize the design of the reactors as well as to determine the best operation conditions for the overall process integration scheme [10,11]. For instance, the correct assessment of relevant design parameters such as minimum residence times or the optimal operation temperatures depend on reliable kinetic modelling. The kinetics driving the carbonation reaction of CaO has been amply investigated due to the technological relevance of this process, encompassing CO_2 capture, cement production and energy storage [10–16]. It is generally agreed that the carbonation reaction of CaO is a complex process composed of two consecutive stages; a very rapid reaction often termed *chemically controlled*, in which a $CaCO_3$ clogging layer forms on the surface of the reacting CaO particles that hinders further carbonation [17–20]. The subsequent *diffusion controlled* stage is limited by the slow-paced counter-current solid-state diffusion of CO_3^{2-} and O^{2-} through this product layer [21]. In an industrial process, the material ought to be transported out of the reactor in a few minutes. Consequently, some authors prefer to restrict the kinetic analysis to the relevant first stage [10,16,22].

Beyond those basic agreements, the kinetic parameters proposed to describe the carbonation reaction in the different studies present significant inconsistencies. For instance, the activation energies published vary in a wide range from 24 to 215 kJ mol^{-1}, depending on experimental conditions such as CO_2 partial pressure, the reaction temperature and even on the type of limestone employed [11,16]. Likewise, the kinetic models used to describe the carbonation reaction vary from simple first and zero-order kinetic models [11,23–25], to significantly more complex ones such as random pore, shrinking core or grain models [26–28]. The latter models take into account microstructural constraints such as initial surface area and pore size distribution, as it has been observed that carbonation kinetics change significantly with the number of cycles due to the sintering-induced morphological and textural changes sustained by the sample in terms of porosity, crystallinity and grain size [29,30]. However, the influence of these parameters is hard to implement in models as they rapidly change with time as the material transforms and sinters. Moreover, the influence of CO_2 partial pressure on carbonation kinetics is particularly relevant nearby the equilibrium temperature. In such situation, the microreversibility principle should be considered, as the reverse decarbonation reaction interferes substantially [31–33].

The lack of a well-accepted model able to describe satisfactorily both carbonation stages in a wide range of experimental conditions has led to the proposal of increasingly complex models that rely on several adjustable fitting parameters to accommodate the experimental data [34–36]. However, before developing complex models, often only valid within a narrow range of experimental conditions, we should first ponder about the reliability of the experimental data. The calcium looping process has been studied through different experimental setups, each of which presents advantages and drawbacks. These include thermogravimetric analysis (TGA), fluidized bed reactors, drop tube reactors, in-situ X-ray diffraction and microfluidized bed thermogravimetric analysis [9,37–41]. Thus, the differences in the large variety of experimental methods and conditions used to study the process also contribute to the discrepancies found in the literature.

This work aims to bring to the forefront the importance of some seldom considered experimental parameters and evaluate their effects in CaO carbonation studies conducted in a thermogravimetric analyzer. Specifically, we aim to demonstrate the remarkable influence the gas flow rate and the reactor volume has on the apparent kinetic parameters derived, to the point of rendering meaningless the results of any kinetic study carried out without considering them. Albeit the study presented here focuses on experiments carried out on a TGA apparatus, those experimental parameters here studied are also important in the different experimental setups used to study CaO carbonation kinetics. Thus, the conclusions could be safely extrapolated to a wide variety of methods and reactor types.

2. Materials and methods

2.1. Materials

A highly pure natural limestone (99.6 wt% $CaCO_3$) from Matagallar quarry (Seville, Spain, 37° 14′ 18.0″ N 4° 53′ 39.3″ W) was employed in our experiments. To avoid mass and heat transfer phenomena, a small mass of $\sim$ 10 mg was employed in all cases. The sample was sieved to obtain particle sizes smaller than 45 μm.

2.2. Experimental

Carbonation experiments with varying flow rate were carried out in a Q5000IR thermogravimetric analyzer (TA Instruments) equipped with a high sensitivity microbalance, and a furnace heated by IR lamps, which allows fast heating rates (up to 300 °C/min). The small volume reactor (21 cm^3) permits quick changes in the atmosphere of the reaction chamber. Due to equipment requirements, a small flow of inert gas (N_2) must be passed constantly through the head of the balance. This gas is mixed in the sample surroundings with the main reactive gas (CO_2). The flow rate of both protecting and reactive gases feeding the reaction chamber were considered when calculating the partial pressure of CO_2 in the sample environment. Thus, the partial pressure of CO_2 for the different experiments was adjusted by varying the ratio of N_2/CO_2 gases feeding the reaction chamber.

Besides, some carbonation experiments were also carried out in a Q600 simultaneous TGA-DTA analyzer (TA Instruments), equipped with a larger reactor chamber.

The CaO carbonation experiments were carried out at isothermal conditions at temperatures nearby the thermodynamic equilibrium. The experimental scheme used in the experiments is described in Fig. 1. Before carbonation, all samples

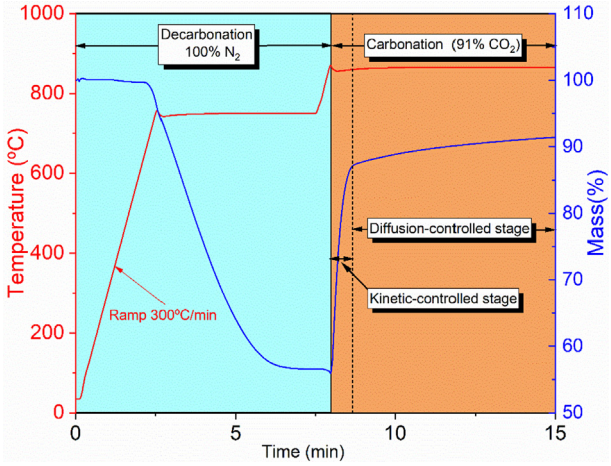

Fig. 1 Example of the experimental scheme used in the carbonation experiments. Starting $CaCO_3$ is heated up to 750 °C under N_2. After a 5-minute calcination isotherm the resulting CaO is heated up to the target carbonation temperature, after which the atmosphere is changed to 91% CO_2. Heating ramps were performed at 300 °C/min.

were pre-calcined by rapidly heating at 300 °C/min from room temperature to 750 °C under pure N_2. After 5-min calcination, samples were heated again up to the selected carbonation temperature. Then the gas atmosphere was immediately switched to achieve the desired partial pressure of CO_2.

2.3. Theory: Carbonation kinetics

The reversible reaction between CaO and CO_2 to produce $CaCO_3$ is the following:

$$CaO_{(s)} + CO_{2(g)} \rightleftharpoons CaCO_{3(s)} \tag{1}$$

As stated above, CaO carbonation takes place in two steps (Fig. 1); a rapid kinetic-controlled stage followed by a much slower diffusion-controlled stage [19]. Firstly, CO_2 molecules are adsorbed on active centers on the surface of the CaO particles in a reversible process whose progress depends on the adsorption and desorption constants and the CO_2 partial pressure in the carbonation environment. Then a reversible chemical reaction follows, leading to the formation of a $CaCO_3$ product layer on the surface of the particles [21]. These two processes altogether constitute the kinetic-controlled stage. Considering the pseudo-steady state hypothesis [42] that establishes that adsorption rate must balance out the reaction rate, and according to the microscopic reversibility principle, it was recently proposed that the reaction rate can be expressed as a function of temperature T and CO_2 partial pressure P as [10]:

$$r(T,P) \approx a_2 e^{-E_2/RT}\left(\frac{P_{CO_2}}{P_{eq}} - 1\right)\left(\frac{1}{\frac{P_{CO_2}}{P_{eq}} + e^{\Delta S_2^0/R} e^{-\Delta H_2^0/RT}}\right) \tag{2}$$

where a_2 is an adjustable preexponential factor, R is the ideal gas constant (8.31 J/K·mol) and E_2 is the carbonation activation energy [10,43]. ΔS_2^0 and ΔH_2^0 are the standard entropy and enthalpy of the second step of the kinetic-controlled reaction phase, which are obtained from the literature as described in [10] (-68 J/(mol·K) and −160 kJ/mol, respectively). The CO_2 partial pressure at equilibrium, P_{eq} , to be used in equation (2), is calculated from thermochemical data as [10]:

$$P_{eq} = 4.083\hat{A} \cdot 10^7 e^{-20474/T(K)} atm \tag{3}$$

As it is inferred from Eq (2), both temperature and pressure have a marked influence on the reaction rate. Besides, the microstructure and morphology of the particles are also relevant [29,42,44]. Therefore, considering all these constraints, the reaction rate can be written as:

$$\frac{dX}{dt} = f(X) r(T,P) \tag{4}$$

where X is the degree of conversion, $f(X)$ is a mechanistic function that considers particles' morphology while $r(T,P)$ covers the dependence of the reaction rate on temperature and pressure as expressed in Eq. (2). A Prout-Tompkins function, $f(X) = X(1\text{-}X)$ can adequately fit the sigmoidal curves typically displayed by carbonation reactions [45]. Due to sintering-induced deactivation and the pore-plugging effect, the maximum attainable CaO conversion during the fast reaction-controlled stage is limited and it further decreases after repeating cycles [46]. Therefore, equation (4) can be modified to take this limitation into account, becoming [10]:

$$\frac{dX}{dt} = X\left(1 - \frac{X}{X_k}\right) r(T,P) \tag{5}$$

where X_k is the value of CaO conversion at the end of the reaction-controlled phase. After integration, Eq (5) leads to:

$$X(t) = \frac{X_k}{1 + e^{-r(t-t_0)}} \tag{6}$$

where t_0 is the time at which conversion in the reaction-controlled reaction is half X_k . Eq (6) can fit reasonably well the experimental data during the fast carbonation stage, thereby allowing the estimation of the term $r(T,P)$ at any given temperature [10]. CaO conversion, X, is typically used to assess the CO_2 capture performance [46]. From experimental data obtained by thermogravimetry, the conversion at any given time obeys the following equation:

$$X(t) = \frac{m - m_i}{m_f - m_i} \tag{7}$$

being m_i the initial mass %, m_f the final mass % and m the sample mass % at an instant time t.

3. Results and discussion.

3.1. Influence of gas flow rate on CaO carbonation kinetics.

In order to assess the influence of the gas flow rate, three sets of isothermal carbonation experiments were run under CO_2 flow rate of 100, 150 and 200 ml/min, respectively. The flow of protective gas through the head of the balance was set at 10, 15 and 20 ml/min, respectively, in order to maintain an environment with 91 vol% CO_2 at atmospheric pressure. The experiments were devised according to the protocol described in Fig. 1, using temperatures of 865, 869, 873, 878 and 883 °C for the isothermal segment. These temperatures were selected to ensure fast carbonation reaction rates nearby the equilibrium temperature, which is 889 °C at the 91 vol% CO_2 concentration under atmospheric pressure used in the

experiments [47]. Fig. 2 compares the time evolution of the CaO conversion at different reaction temperatures. CaO conversion was calculated according to Equation (7). The maximum conversion attained at the end of the reaction-controlled stage under these conditions is about 0.7. Afterwards, carbonation is ruled by the slow diffusion-driven stage. Fig. 2 shows also the best fits of Equation (6) to experimental data on the reaction-controlled part of the carbonation reaction, from which the empirical parameters X_k, r and t_0 are obtained. The parameters derived from these fits for the different experiments are all listed in Table 1. The maximum relative error of the fitting was attained in the case of 100 ml/min and 883 °C, with a mean value of 4%. Several clear-cut conclusions can be drawn from the plots. First, the carbonation reaction at high temperature is very rapid; in most cases the reaction-controlled stage is over in less than 2 min. Therefore, such high temperatures are well suited for any application demanding short residence times. Secondly, the rate of carbonation slows down noticeably as the reaction temperature approaches the equilibrium due to the increasing influence of the reverse reaction. This effect is considered in Equation (2) in the term P_{CO2}/P_{eq}. Finally, curves in Fig. 2 evidence the strong effect the gas flow rate has on the reaction rate; the carbonation rate significantly hastens as the flow rate of CO_2 raises. Actually, the best-fit r values in Table 1 show that the rate constant roughly doubles when the CO_2 flow rate is increased by a factor of 2. Furthermore, the observed increase of the rate constant with the reacting gas flow rate appears even larger at temperatures closer to the equilibrium. That might imply that a high flow rate of CO_2 either suppresses the reverse reaction or promotes the mass transfer. These effects have been observed in other systems [48–50].

The method here employed to perform the kinetic analysis have a distinct advantage; Equation (2) is built upon well-known values of thermodynamic properties with the only exception of a_0, which acts as an adjustable pre-exponential factor. Therefore, any given set of isothermal experiments carried out under similar experimental conditions should all share the pre-exponential a_0 factor. If any experimental parameter not considered in Equation (2), such as the gas flow rate, has any influence on the reaction rate, its effect would be accommodated into the pre-exponential factor. This is demonstrated in Fig. 3a, where the rate constants estimated for the different experimental curves in Fig. 2 are plotted as symbols as a function of the temperature. Equation (2) is then used to construct the theoretical rate constant versus temperature curves (solid lines) that best fit all data points recorded for the same flow rate of CO_2, using a_0 as a fitting parameter. The values of a_2 that provide the best agreement between the experimentally measured rate values and the theoretical curves are listed in Table 2. In a previous work, it was found that $a_0 = 6.9 \cdot 10^4$ min^{-1} led to a good agreement between experimental measurements and theoretical predicitions [10]. However, the set of experiments here studied lead to much larger pre-exponential factors values, named hereafter as a_2 and expressed as a function of the previously proposed a_0. An almost linear relationship can be established between the calculated a_2 and the CO_2 flow rate. Therefore, despite not being explicitly considered in Equation (2), it is clear that the flow rate has a relevant influence on the observed rate constant. As aforementioned, this can be explained by a substantial promotion of mass and heat transfer phenomena.

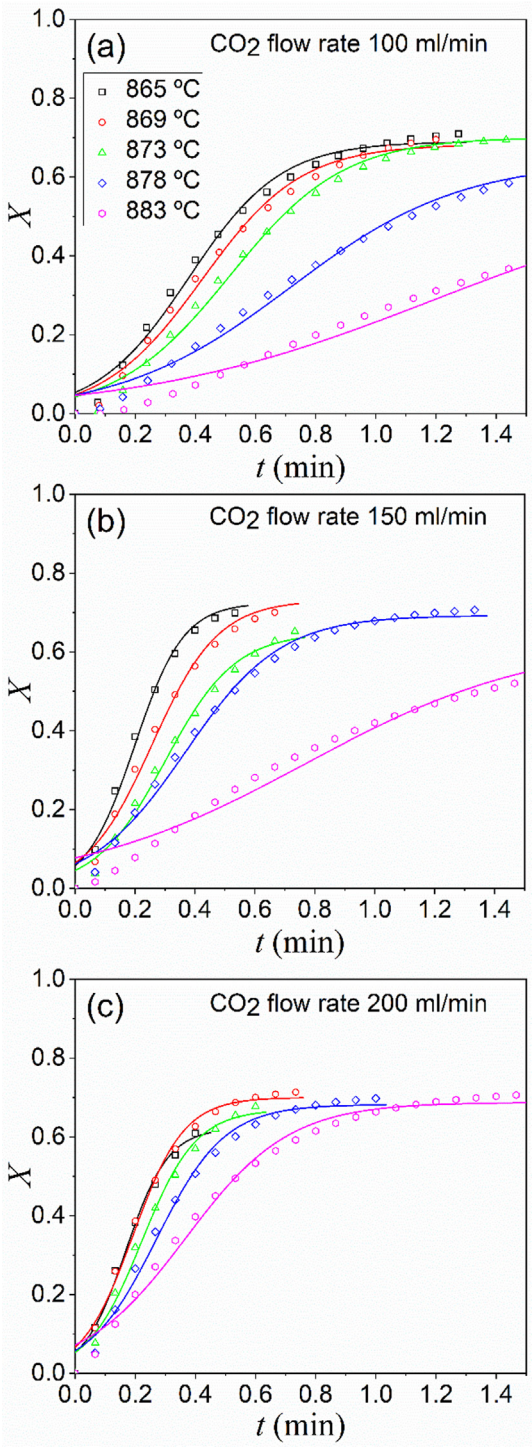

Fig. 2 Time evolution of CaO conversion measured during isothermal carbonation reactionscarried out using (a) 100 ml/min, (b) 150 ml/min and (c) 200 ml/min flow rates of CO_2 at different temperatures. Solid lines correspond to the best fits of Eq. (6) to experimental data.

3.2. Influence of CO_2 partial pressure on CaO carbonation kinetics.

Following the same experimental protocol, a new set of experiments were carried out to measure the time evolution of CaO

Table 1 Best fitting parameters of Eq (6) to experimental data of the time evolution of CaO conversion at different temperatures.

T (C°)	865			869			873			878			883		
CO_2 Flow rate (ml/min)	100	150	200	100	150	200	100	150	200	100	150	200	100	150	200
X_k	0.69 ± 0.01	0.72 ± 0.02	0.62 ± 0.02	0.68 ± 0.01	0.73 ± 0.01	0.70 ± 0.02	0.70 ± 0.02	0.65 ± 0.01	0.67 ± 0.01	0.64 ± 0.01	0.69 ± 0.01	0.68 ± 0.01	0.57 ± 0.01	0.63 ± 0.01	0.69 ± 0.01
$r(min^{-1})$	6.5 ± 0.1	12.3 ± 0.2	14.1 ± 0.2	6.1 ± 0.1	9.1 ± 0.2	11.7 ± 0.1	5.3 ± 0.1	8.6 ± 0.1	11.1 ± 0.2	3.5 ± 0.1	6.3 ± 0.1	8.8 ± 0.1	2.1 ± 0.1	2.6 ± 0.1	5.8 ± 0.2
t_0 (min)	0.38 ± 0.05	0.20 ± 0.03	0.17 ± 0.04	0.42 ± 0.05	0.26 ± 0.03	0.19 ± 0.01	0.52 ± 0.06	0.30 ± 0.03	0.22 ± 0.02	0.72 ± 0.06	0.37 ± 0.03	0.27 ± 0.02	1.18 ± 0.16	0.77 ± 0.11	0.37 ± 0.10

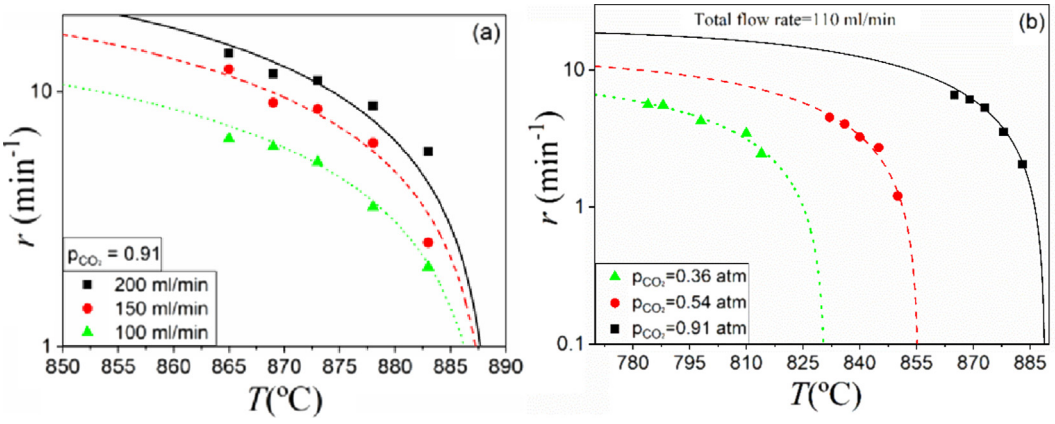

Fig. 3 Carbonation reaction rates measured at different temperatures (symbols) for experiments carried out at (a) different CO_2 flow rates (100, 150 and 200 ml/min as indicated) but identical CO_2 partial pressure of 0.91. (b) Different CO_2 partial pressures (P_{CO2} of 0.36, 0.54 and 0.91 atm as indicated) under a constant overall flow rate of 110 ml/min. Solid lines correspond to the theoretical curves of the reaction rate as determined by equation (2) using the pre-exponential factor a_2 that provides the best agreement with experimental data (indicated, $a_0 = 6.9{\cdot}10^4$ min^{-1}).

Table 2 Details of the experimental conditions used to record each isothermal set of CaO conversion experimental curves (Fig. 3a and 3b), as well as the corresponding a_2 preexponential factor obtained for each set by fitting the measured reaction rate to Equation (2).

CO2 flow rate (ml/min)	100	150	200	40	60	100
N2 flow rate (ml/min)	10	15	20	70	50	10
P_{CO_2} (atm)	0.91			0.36	0.54	0.91
T_{eq} (°C)	888.8			831.4	856.1	888.8
a_2 (1/min)	$(8.4 \pm 0.2){\cdot}10^5$	$(13.2 \pm 0.3) \cdot 10^5$	$(17.2 \pm 0.6) \cdot 10^5$		$(9.1 \pm 0.3){\cdot}10^5$	
$a_0 = 6.9{\cdot}10^4$ 1/min						

conversion by varying N_2/CO_2 ratios in order to assess the influence of CO_2 partial pressure in the reaction environment on the derived pre-exponential factor in Eq. (2). A description of the experimental conditions used can be found in Table 2. In this set of experiments the overall flow rate was maintained constant, but the flow rate of each individual gas was changed. The isothermal curves were analysed, as described in the previous section, to determine the carbonation rate, which are then plotted as a function of reaction temperature (Fig. 3b). As shown in Fig. 3b, theoretical r-T plots constructed assuming the same a_2 value of $9.1{\cdot}10^5$ min^{-1} can properly fit all experimental data points, regardless the partial pressure under which the experiments were carried out. This demonstrates that when the overall flow rate is fixed, the relationship between the reaction rate, P_{CO2} and temperature can be established through the same pre-exponential factor. Moreover, it strengthens the

argument in the previous section that the enhancement of the reaction rate at higher flow rates was due to the promotion of mass and heat transfer phenomena.

3.3. Influence of the reactor's volume on CaO carbonation kinetics

Given the relevance of both the CO_2 flow rate and partial pressure on the carbonation rate, the reactor's volume must necessarily play a major role that needs to be considered when analysing data from carbonation experiments. For instance, it is usual to trigger CaO carbonation by quickly switching the atmosphere from inert to a CO_2-rich atmosphere. However, such atmosphere swings are very complex to implement, as the displacement of the prior gas is far from being instantaneous. Therefore, the larger the ratio reactor chamber volume to displacing gas flow rate, the longer the time needed to attain the desired gas composition in the reactor chamber. To demonstrate this, two carbonation experiments were carried out under isothermal conditions at 850 °C in two different thermogravimetric analyzers, namely, Q600 and Q5000IR (both from TA Instruments). According to the equipment specifications, the Q600 and Q5000IR have a volume of 71 cm^3 and 21 cm^3, respectively. The sample was initially heated up to 850 °C in N_2. Then, the incoming gas was switched to CO_2. The incoming flow rate was set at 100 ml/min. The obtained results are shown in Fig. 4. The reaction-controlled carbonation phase is completed in just a few seconds for the sample carbonated in the Q5000IR instrument, whereas just partial carbonation is reached in several minutes in the Q600 analyzer. Not only the shape of the conversion curve changes radically, but also the maximum conversion attained. This is a consequence of the time needed to reach a homogeneous gas atmosphere in each instrument. The smaller volume of the Q5000IR analyzer allows a rapid change of atmosphere, reaching the desired CO_2 partial pressure in a short time, and thus carbonation proceeds faster under the target conditions. On the other hand, in the reactor with the larger volume of the Q600 analyzer the CO_2 partial pressure slowly increases while the reaction is still underway. As the shape of the conversion curve contains information related to the reaction mechanism [51], this implies that the kinetic description obtained from a set of experiments would be completely different depending on the equipment used.

In order to simulate the gradual enrichment in CO_2 during the filling of the reactor, several experiments were performed using different gas filling rates in the low-volume reaction chamber of the Q5000IR analyzer. Limestone samples were calcined in N_2 and then quickly heated up to 885 °C. Then, the flowing gas was changed to CO_2 while maintaining the temperature constant. Instead of feeding the reaction chamber with a constant flow rate of CO_2, the flow rate was linearly increased from 25 ml/min to 200 ml/min at six different ramp rates, ranging from 2 ml/min^2 to 200 ml/min^2. Fig. 5a details all the different gas filling ramps programmed. Fig. 5b presents the time evolution of CaO conversion measured as a function of time. A clear correlation exists between the CO_2 filling rate, the progress of the reaction and the shape of the conversion-time curves. These results match the conversion-time profiles obtained in the experiments carried out in reactors with different volumes (Fig. 4). The wider conversion-time profiles (Fig. 5b) observed at slow gas filling rates is a consequence of the reduced initial carbonation rate due to the low CO2 partial pressure (P_{CO2}) in the reaction chamber. As P_{CO2} rises, the reaction accelerates (Fig. 5c). This is also illustrated in Fig. 6a and 6b, which compares the CaO conversion curves, the flow rate and the estimated partial pressure of CO_2 as a function of time obtained in the experiments carried out using the fastest and the slowest gas filling rates (200 ml/min^2 and 2 ml/min^2, respectively). For the sake of clarity, the value of the equilibrium partial pressure at 885 °C (P_{eq} = 0.86 atm) has been indicated in these graphs. Thus, the reaction starts when that value is overcome. It is evident that P_{CO2} rises nonlinearly and the time needed to attain the desired P_{CO2} concentration in the reaction chamber strongly depends on the filling rate. This value of P_{co2} is 0.95 because a cover N_2 flow was maintained of 10 ml/min to protect the balance.

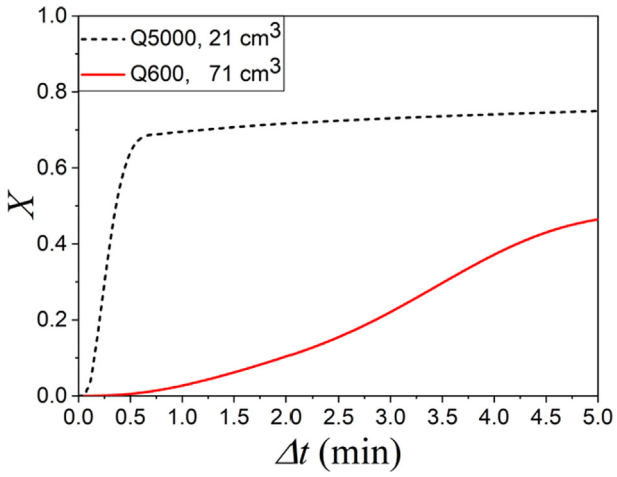

Fig. 4 - Time evolution of CaO conversion X(t) during carbonation isotherms registered in two instruments with reaction chambers with different volume. Carbonation was carried out in CO_2 at a temperature of 850 °C and a CO_2 flow rate of 100 ml/min.

To illustrate the effect of a time dependent P_{CO2}, the curves were analyzed using Equation (2) as in previous sections. The best-fitting parameters are listed in Table 3. As could be expected from Fig. 5b, the value of X_k decreases with the gas filling rate, alongside the rate of the reaction. Curves in Fig. 5b also show a lag between the time the P_{CO2} is high enough to favor carbonation over calcination and the time CaO starts to convert into $CaCO_3$. At 885 °C, as has been said, the equilibrium pressure of CO_2 is 0.86 atm. Some authors have previously reported that the reaction starts after an induction or nucleation period [15,52,53]. This induction period has been modeled and used to estimate residence times for practical purposes. While the results here reported should not be used to claim that the induction period is an artifact, it is evident that "artificially" long induction times appear when experimental conditions are not carefully controlled.

Fig. 6c depicts the actual CaO conversion attained by the time the CO_2 partial pressure reaches the target value of 0.95 atm as a function of the filling rate. As it can be seen, even in the most favorable case, a nonnegligible fraction of the CaO

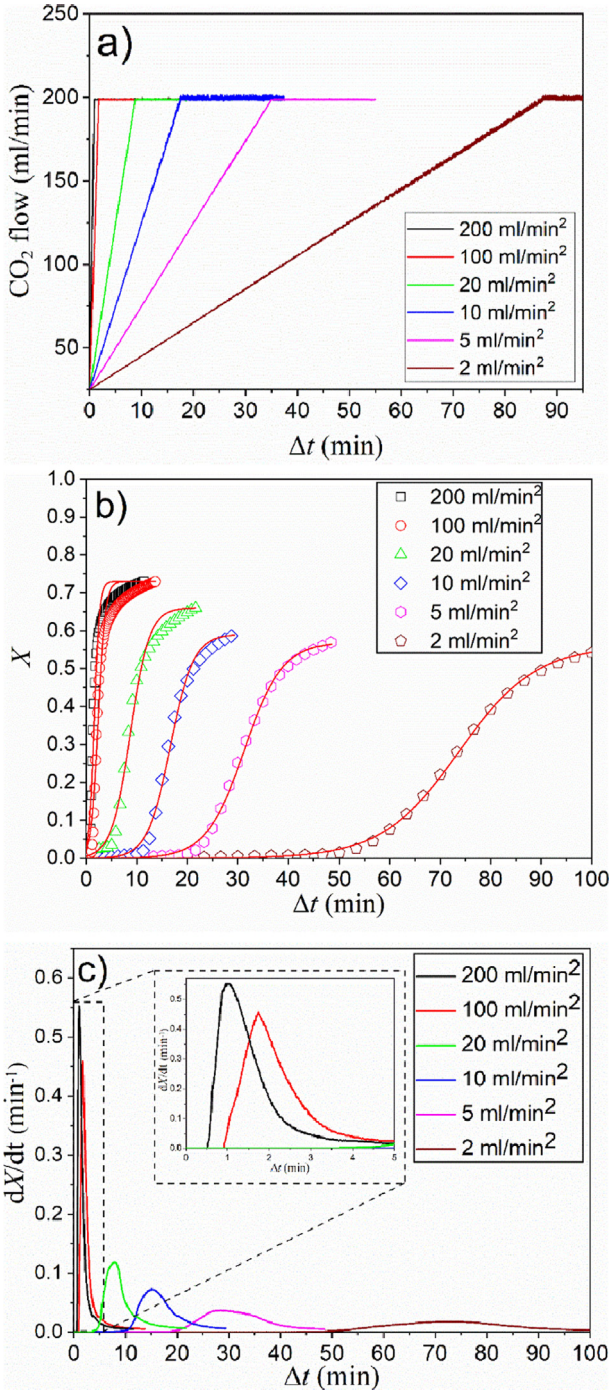

Fig. 5 Time evolution of (a) CO_2 flow rate, (b) CaO conversion and (c) Reaction rate recorded during carbonation experiments performed using CO_2 filling rates (from 2 ml/min^2 to 200 ml/min^2, as detailed in (a)) and a constant temperature of 885 °C. Solid lines in (b) correspond to the best fits of equation 8 to experimental data.

has already reacted before $P_{CO_2} = 0.95$ is attained. For slower filling rates, the reaction might be finished well before it. Therefore, a proper kinetic analysis based on equations considering P_{co2} should consider this effect to avoid significant misleadings.

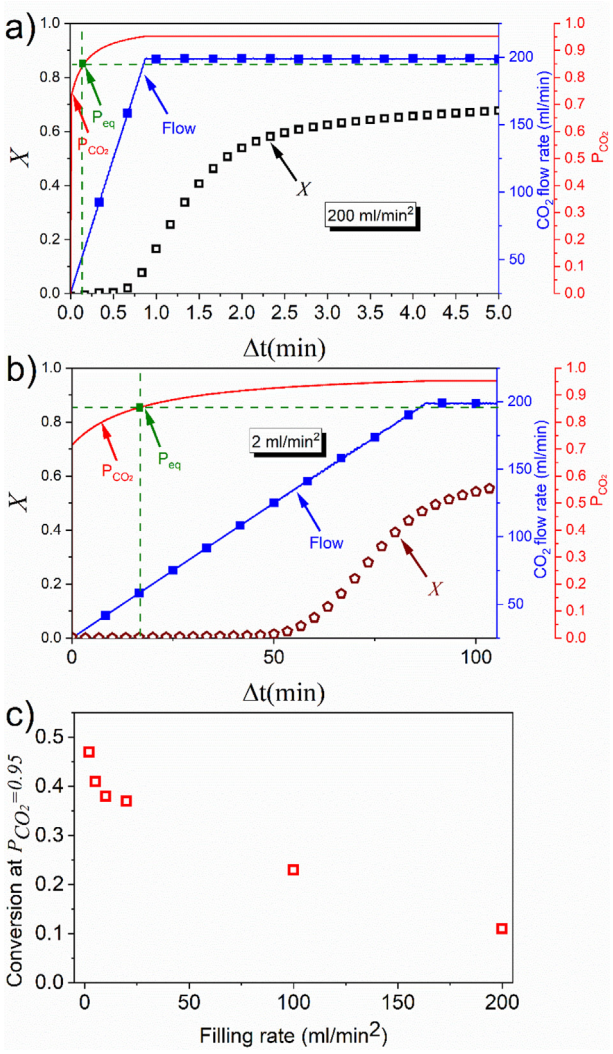

Fig. 6 CaO conversion curves obtained during carbonation in the Q5000IR analyzer by filling the reaction chamber using CO_2 flow ramps of (a) 200 ml/min^2 and (b) 2 ml/min^2 (from 25 ml/min to 200 ml/min) at 885 °C. Open symbols correspond to data on conversion (X). Blue line and filled blue squares correspond to CO_2 flow rate. The red line in b corresponds to the time evolution of P_{CO_2} . c) CaO conversion attained when the CO2 partial pressure target ($P_{CO_2} = 0.95$) is reached a function of the filling rate. The value of the equilibrium partial pressure at 885 °C (P_{eq} = 0.86 atm) has been indicated in (a) and (b).

4. Conclusions

In this work, our main goal has been to draw the attention to seldom-considered experimental parameters that can strongly condition the analysis of CaO carbonation kinetics when carried out in conditions nearby equilibrium, at high temperature and CO_2-rich atmospheres. The kinetics of CaO carbonation under these conditions has been amply studied due to its interest in CO_2 capture and thermochemical energy storage applications.

The results here presented demonstrate that the reaction rate is strongly affected by the CO_2 flow rate, CO_2 partial pressure and the volume of the reaction chamber. For instance,

Table 3 Reaction rates, "apparent" induction period and X_k values obtained from experiments using different CO2 filling rates.

CO2 Flow ramp rates (ml/min^2)	200	100	20	10	5	2
r (1/min)	1.93 ±0.06	1.42 ±0.07	0.53 ±0.05	0.44±0.03	0.27 ±0.02	0.13 ±0.01
Induction period (min)	–	–	–	≈5	≈10	≈40
X_k	0.72 ±0.01	0.72 ±0.01	0.66 ±0.02	0.59 ±0.01	0.57 ±0.01	0.56 ±0.02

high gas flow rates promote mass and heat transfer mechanisms speeding the carbonation process and helping overcome the hindering effect of the reverse reaction. More importantly, it has been proven that the volume of the reactor is a critical parameter as it is very difficult to achieve in practice a sufficiently fast transition from inert to the target reactive gas atmosphere as to neglect the extent of CaO conversion attained before the desired conditions are reached. If the CO_2 flow rate is not high enough as depending on the reactor volume, the carbonation reaction would not occur at a constant CO_2 partial pressure, but under a rising, time dependent P_{CO2} profile instead. As a result, the rate constants, the maximum attained conversion and the shape of the conversion-time curves would depend on the flow rate, thereby denying the results of any kinetic analysis. These observations might explain the significant discrepancies in published results as the kinetic parameters obtained would be dependent on the design of the reactor and on the experimental conditions employed. The implications of such bogus results can be important since a proper kinetic modelling of the carbonation reaction is a crucial step in the design of the large-scale reactors. In summary, the comprehension of such a complex system requires an integral approach comprising all kinetic, thermodynamic and reactor design parameters if a kinetic description with predictive capabilities beyond the experimental set-up limitations is pursued. Even though this study has been focused on the CaO carbonation reaction similar constraints might well be present in other gas–solid reactions.

Declaration of Competing Interest

The authors declare that they have no known competing financial interests or personal relationships that could have appeared to influence the work reported in this paper.

Acknowledgements

This work has been supported by the European Union's research and innovation program Horizon 2020 under grant agreement No. 727348, project SOCRATCES. We also acknowledge the funding received by the Spanish Government Agency Ministerio de Economía y Competitividad and FEDER (projects CTQ2017-83602-C2-1-R and CTQ2017-83602-C2-2-R) and by Junta de Andalucía-Consejería de Economía, Conocimiento, Empresas y Universidad and FEDER (projects P18-FR-1087 and US-1262507). Financial support from project 201960E092 (INTRAMURAL-CSIC) is also acknowledged.

References

[1] K. Dong, X. Dong, C. Dong, Determinants of the global and regional CO2 emissions: What causes what and where?, Appl Econ. 51 (46) (2019) 5031–5044, https://doi.org/10.1080/00036846.2019.1606410.

[2] M.E. Boot-Handford, J.C. Abanades, E.J. Anthony, M.J. Blunt, S. Brandani, N. Mac Dowell, J.R. Fernández, M.-C. Ferrari, R. Gross, J.P. Hallett, R.S. Haszeldine, P. Heptonstall, A. Lyngfelt, Z. Makuch, E. Mangano, R.T.J. Porter, M. Pourkashanian, G. T. Rochelle, N. Shah, J.G. Yao, P.S. Fennell, Carbon capture and storage update, Energy Environ. Sci. 7 (1) (2014) 130–189, https://doi.org/10.1039/C3EE42350F.

[3] Hanak DP, Anthony EJ, Manovic V. A review of developments in pilot-plant testing and modelling of calcium looping process for CO < inf > 2 < /inf > capture from power generation systems. Energy Environ Sci 2015;8:2199–249. https://doi.org/10.1039/c5ee01228g.

[4] J.C. Abanades, B. Arias, A. Lyngfelt, T. Mattisson, D.E. Wiley, H. Li, M.T. Ho, E. Mangano, S. Brandani, Emerging CO2 capture systems, Int. J. Greenh Gas Control 40 (2015) 126–166, https://doi.org/10.1016/j.ijggc.2015.04.018.

[5] C. Ortiz, J.M. Valverde, R. Chacartegui, L.A. Perez-Maqueda, P. Giménez, The Calcium-Looping (CaCO3/CaO) process for thermochemical energy storage in Concentrating Solar Power plants, Renew. Sustain. Energy Rev. 113 (2019) 109252, https://doi.org/10.1016/j.rser.2019.109252.

[6] SOCRATCES (SOlar Calcium-looping integRAtion for ThermoChemical Energy Storage); n.d. https://socratces.eu/ (accessed November 23, 2020).

[7] R. Chacartegui, A. Alovisio, C. Ortiz, J.M. Valverde, V. Verda, J.A. Becerra, Thermochemical energy storage of concentrated solar power by integration of the calcium looping process and a CO2 power cycle, Appl. Energy 173 (2016) 589–605, https://doi.org/10.1016/j.apenergy.2016.04.053.

[8] B. Sarrion, J.M. Valverde, A. Perejon, L. Perez-Maqueda, P.E. Sanchez-Jimenez, On the Multicycle Activity of Natural Limestone/Dolomite for Thermochemical Energy Storage of Concentrated Solar Power, Energy Technol. 4 (8) (2016) 1013–1019, https://doi.org/10.1002/ente.201600068.

[9] J. Arcenegui-Troya, P.E. Sánchez-Jiménez, A. Perejón, J.M. Valverde, R. Chacartegui, L.A. Pérez-Maqueda, Calcium-Looping Performance of Biomineralized CaCO < inf > 3 < /inf > for CO < inf > 2 < /inf > Capture and Thermochemical Energy Storage, Ind. Eng. Chem. Res. 59 (2020), https://doi.org/10.1021/acs.iecr.9b05997.

[10] C. Ortiz, J.M. Valverde, R. Chacartegui, L.A. Perez-Maqueda, Carbonation of Limestone Derived CaO for Thermochemical Energy Storage: From Kinetics to Process Integration in Concentrating Solar Plants, ACS Sustain. Chem. Eng. 6 (5) (2018) 6404–6417, https://doi.org/10.1021/acssuschemeng.8b00199.

[11] S.A. Salaudeen, B. Acharya, A. Dutta, CaO-based CO2 sorbents: A review on screening, enhancement, cyclic stability, regeneration and kinetics modelling, J. CO2 Util 23 (2018) 179–199, https://doi.org/10.1016/j.jcou.2017.11.012.
[12] D. LEE, An apparent kinetic model for the carbonation of calcium oxide by carbon dioxide, Chem. Eng. J. 100 (1-3) (2004) 71–77, https://doi.org/10.1016/j.cej.2003.12.003.
[13] Z. Zhou, P. Xu, M. Xie, Z. Cheng, W. Yuan, Modeling of the carbonation kinetics of a synthetic CaO-based sorbent, Chem. Eng. Sci. 95 (2013) 283–290, https://doi.org/10.1016/j.ces.2013.03.047.
[14] H. Wang, Z. Li, Y.e. Li, N. Cai, Reduced-order model for CaO carbonation kinetics measured using micro-fluidized bed thermogravimetric analysis, Chem. Eng. Sci. 229 (2021) 116039, https://doi.org/10.1016/j.ces.2020.116039.
[15] A. Di Giuliano, K. Gallucci, P.U. Foscolo, Determination of Kinetic and Diffusion Parameters Needed to Predict the Behavior of CaO-Based CO2 Sorbent and Sorbent-Catalyst Materials, Ind. Eng. Chem. Res. 59 (15) (2020) 6840–6854, https://doi.org/10.1021/acs.iecr.9b05383.
[16] J. Fuchs, S. Müller, J.C. Schmid, H. Hofbauer, A kinetic model of carbonation and calcination of limestone for sorption enhanced reforming of biomass, Int. J. Greenh. Gas Control 90 (2019) 102787, https://doi.org/10.1016/j.ijggc.2019.102787.
[17] D. Alvarez, J.C. Abanades, Determination of the critical product layer thickness in the reaction of CaO with CO2, Ind. Eng. Chem. Res. 44 (15) (2005) 5608–5615, https://doi.org/10.1021/ie050305s.
[18] M. Benitez-Guerrero, B. Sarrion, A. Perejon, P.E. Sanchez-Jimenez, L.A. Perez-Maqueda, J. Manuel Valverde, Large-scale high-temperature solar energy storage using natural minerals, Sol. Energy Mater. Sol. Cells 168 (2017) 14–21, https://doi.org/10.1016/j.solmat.2017.04.013.
[19] J.C. Abanades, D. Alvarez, Conversion limits in the reaction of CO2 with lime, Energy Fuels 17 (2) (2003) 308–315, https://doi.org/10.1021/ef020152a.
[20] Sarrión B, Perejón A, Sánchez-Jiménez PE, Pérez-Maqueda LA, Valverde JM. Role of calcium looping conditions on the performance of natural and synthetic Ca-based materials for energy storage. J CO2 Util 2018;28:374–84. https://doi.org/10.1016/j.jcou.2018.10.018.
[21] BERUTO D, BARCO L, SEARCY AW. CO2-Catalyzed Surface Area and Porosity Changes in High-Surface-Area CaO Aggregates. J. Am. Ceram. Soc. 1984. https://doi.org/10.1111/j.1151-2916.1984.tb19644.x.
[22] J. Yang, L. Ma, H. Liu, Y.i. Wei, B. Keomounlath, Q. Dai, Thermodynamics and kinetics analysis of Ca-looping for CO2 capture: Application of carbide slag, Fuel 242 (2019) 1–11, https://doi.org/10.1016/j.fuel.2019.01.018.
[23] P. Sun, J.R. Grace, C.J. Lim, E.J. Anthony, Determination of intrinsic rate constants of the CaO-CO2 reaction, Chem. Eng. Sci. 63 (1) (2008) 47–56, https://doi.org/10.1016/j.ces.2007.08.055.
[24] S.A. Stevenson, Thermodynamic considerations in CO2 utilization, AIChE J. 65 (9) (2019), https://doi.org/10.1002/aic.v65.910.1002/aic.16695.
[25] J. Yin, C. Qin, B.o. Feng, L. Ge, C. Luo, W. Liu, H. An, Calcium looping for CO2 capture at a constant high temperature, Energy Fuels 28 (1) (2014) 307–318, https://doi.org/10.1021/ef401399c.
[26] Z. Li, General rate equation theory for gas–solid reaction kinetics and its application to CaO carbonation, Chem. Eng. Sci. 227 (2020) 115902, https://doi.org/10.1016/j.ces.2020.115902.
[27] G. Grasa, R. Murillo, M. Alonso, J.C. Abanades, Application of the random pore model to the carbonation cyclic reaction, AIChE J 55 (5) (2009) 1246–1255, https://doi.org/10.1002/aic.v55:510.1002/aic.11746.
[28] A. Scaltsoyiannes, A. Antzaras, G. Koilaridis, A. Lemonidou, Towards a generalized carbonation kinetic model for CaO-based materials using a modified random pore model, Chem. Eng. J. 407 (2021) 127207, https://doi.org/10.1016/j.cej.2020.127207.
[29] J.D. Durán-Martín, P.E. Sánchez Jimenez, J.M. Valverde, A. Perejón, J. Arcenegui-Troya, P. García Triñanes, L.A. Pérez Maqueda, Role of particle size on the multicycle calcium looping activity of limestone for thermochemical energy storage, J. Adv. Res. 22 (2020) 67–76, https://doi.org/10.1016/j.jare.2019.10.008.
[30] W. Liu, B. González, M.T. Dunstan, D. Saquib Sultan, A. Pavan, C.D. Ling, C.P. Grey, J.S. Dennis, Structural evolution in synthetic, Ca-based sorbents for carbon capture, Chem. Eng. Sci. 139 (2016) 15–26, https://doi.org/10.1016/j.ces.2015.09.016.
[31] J.M. Criado, M. González, J. Málek, A. Ortega, The effect of the CO2 pressure on the thermal decomposition kinetics of calcium carbonate, Thermochim. Acta 254 (1995) 121–127, https://doi.org/10.1016/0040-6031(94)01998-V.
[32] A. Perejón, P.E. Sánchez-Jiménez, J.M. Criado, L.A. Pérez-Maqueda, Magnesium hydride for energy storage applications: The kinetics of dehydrogenation under different working conditions, J. Alloys Compd 681 (2016) 571–579, https://doi.org/10.1016/j.jallcom.2016.04.191.
[33] M. Maciejewski, A. Reller, How (UN)reliable are kinetic data of reversible solid-state decomposition processes?, Thermochim Acta 110 (1987) 145–152, https://doi.org/10.1016/0040-6031(87)88221-7.
[34] M. Li, H. Yang, L. Song, Y. Wu, Dynamic Coupling of Pore Structure Evolution with Carbonation Kinetics of CaO-Based Sorbents: Experiments and Modeling, Energy Fuels 31 (11) (2017) 12466–12476, https://doi.org/10.1021/acs.energyfuels.7b02196.
[35] A. Benedetti, M. Strumendo, Application of a random pore model with distributed pore closure to the carbonation reaction, Chem. Eng. Trans. (2015), https://doi.org/10.3303/CET1543193.
[36] J. Cai, S. Wang, C. Kuang, Modeling of carbonation reaction for CaO-based limestone with CO2 in multitudinous calcination-carbonation cycles, Int. J. Hydrogen Energy 42 (31) (2017) 19744–19754, https://doi.org/10.1016/j.ijhydene.2017.06.173.
[37] J.G. Yao, Z. Zhang, M. Sceats, G.C. Maitland, P.S. Fennell, Two-Phase Fluidized Bed Model for Pressurized Carbonation Kinetics of Calcium Oxide, Energy Fuels 31 (10) (2017) 11181–11193, https://doi.org/10.1021/acs.energyfuels.7b01384.
[38] S. Turrado, B. Arias, J.R. Fernández, J.C. Abanades, Carbonation of Fine CaO Particles in a Drop Tube Reactor, Ind. Eng. Chem. Res. 57 (40) (2018) 13372–13380, https://doi.org/10.1021/acs.iecr.8b02918.
[39] A. Biasin, C.U. Segre, G. Salviulo, F. Zorzi, M. Strumendo, Investigation of CaO–CO2 reaction kinetics by in-situ XRD using synchrotron radiation, Chem. Eng. Sci. 127 (2015) 13–24, https://doi.org/10.1016/j.ces.2014.12.058.
[40] Y. Li, Z. Li, H. Wang, N. Cai, CaO carbonation kinetics determined using micro-fluidized bed thermogravimetric analysis, Fuel 264 (2020), https://doi.org/10.1016/j.fuel.2019.116823 116823.
[41] M. Alonso, Y.A. Criado, J.C. Abanades, G. Grasa, Undesired effects in the determination of CO2 carrying capacities of CaO during TG testing, Fuel 127 (2014) 52–61, https://doi.org/10.1016/j.fuel.2013.08.005.
[42] M. Pijolat, L. Favergeon, Kinetics and Mechanisms of Solid-Gas Reactions, Handb. Therm. Anal. Calorim. (2018), https://doi.org/10.1016/B978-0-444-64062-8.00011-5.
[43] C.T. Campbell, J.R.V. Sellers, The entropies of adsorbed molecules, J. Am. Chem. Soc. 134 (43) (2012) 18109–18115, https://doi.org/10.1021/ja3080117.
[44] D. Alvarez, J.C. Abanades, Pore-size and shape effects on the recarbonation performance of calcium oxide submitted to

repeated calcination/recarbonation cycles, Energy Fuels 19 (1) (2005) 270–278, https://doi.org/10.1021/ef049864m.

[45] M.E. Brown, The Prout-Tompkins rate equation in solid-state kinetics, Thermochim. Acta 300 (1-2) (1997) 93–106, https://doi.org/10.1016/S0040-6031(96)03119-X.

[46] P.E. Sanchez-Jimenez, J.M. Valverde, L.A. Perez-Maqueda, Multicyclic conversion of limestone at Ca-looping conditions: The role of solid-sate diffusion controlled carbonation, Fuel 127 (2014) 131–140, https://doi.org/10.1016/j.fuel.2013.09.064.

[47] J.M. Valverde, P.E. Sanchez-Jimenez, L.A. Perez-Maqueda, Limestone calcination nearby equilibrium: Kinetics, CaO crystal structure, sintering and reactivity, J. Phys. Chem. C 119 (4) (2015) 1623–1641, https://doi.org/10.1021/jp508745u.

[48] B.M. Dodd, H.V. Tafreshi, G.C. Tepper, Flow-enhanced kinetics of uranyl (UO2) transport into nano-porous silica gel, Mater. Des. 106 (2016) 330–335, https://doi.org/10.1016/j.matdes.2016.05.107.

[49] S.Y. Joshi, M.P. Harold, V. Balakotaiah, Overall mass transfer coefficients and controlling regimes in catalytic monoliths, Chem. Eng. Sci. 65 (5) (2010) 1729–1747, https://doi.org/10.1016/j.ces.2009.11.021.

[50] W. Liu, J. Yin, C. Qin, B.o. Feng, M. Xu, Synthesis of CaO-based sorbents for CO2 capture by a spray-drying technique, Environ. Sci. Technol. 46 (20) (2012) 11267–11272, https://doi.org/10.1021/es301783b.

[51] P.E. Sánchez-Jiménez, L.A. Pérez-Maqueda, A. Perejón, J.M. Criado, Generalized kinetic master plots for the thermal degradation of polymers following a random scission mechanism, J. Phys. Chem. A 114 (30) (2010) 7868–7876, https://doi.org/10.1021/jp103171h.

[52] L. Rouchon, L. Favergeon, M. Pijolat, Analysis of the kinetic slowing down during carbonation of CaO by CO 2, J. Therm. Anal. Calorim. 113 (3) (2013) 1145–1155, https://doi.org/10.1007/s10973-013-2950-5.

[53] Z. Li, H. Sun, N. Cai, Rate equation theory for the carbonation reaction of CaO with CO 2, Energy Fuels 26 (7) (2012) 4607–4616, https://doi.org/10.1021/ef300607z.